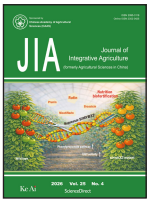
Journal of Integrative Agriculture 2026, 25(4): 1636–1646

Available online at ScienceDirect

Journal of Integrative Agriculture



RESEARCH ARTICLE

Identification of broad-spectrum B-cell and T-cell epitopes of H9 subtype avian influenza virus HA protein using polypeptide scanning

Keji Quan[1*], Nan Zhang[1*], Mengqi Lin[1], Yuan Liu[1], Yue Li[1], Qun Hu[1], Maoshun Nie[1], Tao Qin[1, 2, 3], Jingzhi Li[4], Hongwei Ma[4], Sujuan Chen[1, 2, 3#], Daxin Peng[1, 2, 3#], Xiufan Liu[1, 2, 3]

[1] *College of Veterinary Medicine, Yangzhou University/Jiangsu Co-Innovation Center for the Prevention and Control of Important Animal Infectious Disease and Zoonoses, Yangzhou 225009, China*

[2] *Joint International Research Laboratory of Agriculture and Agri-Product Safety, Ministry of Education, Yangzhou 225009, China*

[3] *Jiangsu Research Centre of Engineering and Technology for Prevention and Control of Poultry Disease, Yangzhou 225009, China*

[4] *Division of Nanobiomedicine, Suzhou Institute of Nano-Tech and Nano-Bionics, Chinese Academy of Sciences, Suzhou 215000, China*

Highlights

- The B-cell and T-cell epitopes of the HA1 protein in H9N2 avian influenza virus were identified by peptide scanning.
- Peptides H9-21, H9-26, and H9-30 were identified as conserved B-cell epitopes.
- Peptides H9-15, H9-22, and H9-23 were recognized as cross-reactive T-cell epitopes.

Abstract

The H9N2 subtype avian influenza virus (AIV) hemagglutinin (HA) protein is a major immunogen in which HA1 is a genetic variant and HA2 is relatively conserved. Identifying broad-spectrum antigen epitopes targeting HA1 is crucial for vaccine design and detection. Based on the phylogenetic and serological analyses, we identified 2 antigenic groups and 3 representative viruses: A/chicken/Jiangsu/JY040218C/2019, A/pigeon/Jiangsu/JY020616/2019, and A/chicken/Jiangsu/WX090312/2018. An overlapping peptide library was synthesized using HA1 amino acid sequences of the viruses as templates. Through peptide scanning of the sera against different strains of H9N2 subtype AIV, we identified peptides from 4 regions (H9-2/3, H9-20/21, H9-26, and H9-29/30/31) that demonstrated broad-spectrum reactivity. Immunological assay results demonstrated that H9-21 (^{219}RIFKPLIGPRPLVNGLMGRI^{239}), H9-26 (^{269}SGESHGRILKTDLKMGSCTV^{289}), and H9-30 (^{309}YAFGNCPKYI GVKSLKLAVG^{329}) effectively induced antibody generation and conferred partial protective efficacy against the parent virus JY040218C. The results of lymphocyte proliferation and ELISpot assays indicated that peptides H9-15 (^{159}MRWLTQKNNAYPTQDAQYTN^{179}), H9-22 (^{229}PLVNGLMGRINYYWSVLKP G^{249}), and H9-23 (^{239}NYYWSVLKPGQTLRIKSDGN^{259}) could effectively stimulate the expression of interferon-gamma in peripheral blood lymphocytes of chickens immunized against different strains of H9N2 AIV. Collectively, 5 novel cell epitopes H9-15, H9-22, H9-23, H9-26, and H9-30, including the best B cell epitope H9-26 and the best T cells epitope H9-22, were identified that could be targeted for vaccine design or detection approaches against H9N2 AIVs.

Keywords: H9N2 subtype avian influenza virus, HA protein, epitope, microarray, peptide

1. Introduction

The H9N2 subtype of avian influenza virus (AIV) has been present in China for more than three decades and is commonly found in poultry, with occasional reports of infections in mammals and humans (Li *et al.* 2019), and has led to significant economic loss. Studies indicate that H9N2 acts as a reservoir for internal genes, which could help raise novel AIV strains, such as H7N9, H10N8, and H5N6 (Chen *et al.* 2014; Pu *et al.* 2015; Bi *et al.* 2020). This creates a scenario in which recombinant AIVs can emerge and evolve,

Received 27 February 2024; Received in revised form 30 April 2024; Accepted 22 May 2025; Available online 4 July 2024
Keji Quan, E-mail: DZ120190004@yzu.edu.cn; Nan Zhang, E-mail: DZ120210023@stu.yzu.edu.cn; #Correspondence Sujuan Chen, E-mail: chensj@yzu.edu.cn; Daxin Peng, E-mail: pengdx@yzu.edu.cn
*These authors contributed equally to this work.

© 2026 CAAS. Publishing services by Elsevier B.V. on behalf of KeAi Communications Co. Ltd. This is an open access article under the CC BY-NC-ND license (http://creativecommons.org/licenses/by-nc-nd/4.0/). Peer review under responsibility of Editorial Board of *Journal of Integrative Agriculture*.
doi: 10.1016/j.jia.2024.07.005

thus posing an ongoing public health risk (Liu *et al.* 2014).

The H9N2 subtype of AIV is more commonly observed in clinical cases than the other AIV subtypes. According to the phylogenetic analysis of the hemagglutinin (HA) gene, H9N2 AIV can be categorized into 2 distinct phylogeographic lineages: Eurasia and North America. The North American branch of the H9N2 subtype of AIV is predominantly found in migratory birds, although reports exist of turkeys being infected with this subtype (Peacock *et al.* 2019). In contrast, the Eurasian lineage of the H9N2 subtype of AIV has established at least 3 stable poultry lineages: A/quail/Hong Kong/G1/1997 (G1 like), A/chicken/Beijing/1/94 (BJ94 like, Y280, or G9), and A/chicken/Hong Kong/Y439/1997 (Y439 like) (Guo *et al.* 2000; Zhang *et al.* 2022). A numbering system for global H9-HA fragments was proposed by Liu and Chen (2009), who divided the H9-AIV lineage into 4 sub-lineages (H9.1–H9.4) and subsequently divided them into branches and subbranches. In China, H9.4.2.5 is the most prevalent branch of H9N2 AIV, which underwent differentiation from 2012 to 2013, giving rise to 3 evolutionary branches (C1–C3). Currently, all 3 strains circulate simultaneously, there is a noticeable clustering phenomenon in the antigenicity of these strains, indicating that they have distinct antigenic profiles (Bi *et al.* 2020; Zhang *et al.* 2023; Liang *et al.* 2024). Although China has approved more than 20 commercial vaccine strains since the first H9N2 subtype avian influenza inactivated vaccine (strain A/Chicken/Shanghai/F/98) was approved in 2002, H9N2 AIV is susceptible to antigenic variations owing to vaccine immune pressure (Cao *et al.* 2022). According to the hemagglutination inhibition (HI) and micro-neutralization (MN) results, the H9N2 AIV isolates belong to antigenic groups that differ from those of the vaccines. Additionally, immunoprotection results indicate that the currently used vaccine strains are insufficient to protect poultry against infection by circulating strains (Belser *et al.* 2020; Zhang *et al.* 2023; Zhao *et al.* 2023). Therefore, owing to the highly variable nature of H9N2 AIV, a single inactivated vaccine is no longer sufficient for prevention and control. Therefore, novel broad-spectrum H9N2 subtypes need to be developed for avian influenza vaccines.

Antigenic epitopes are essential for combating AIV. They serve as critical targets for creating universal influenza virus vaccines, developing immune detection techniques, and understanding the immune response mechanisms against AIV. Unlike conformational epitopes, linear epitopes consist of a continuous amino acid sequence and are influenced by their primary structure, which affects their functionality. Recent studies on the linear epitope landscape of the Spike protein of SARS-CoV-2 suggest that a correlation exists between linear epitope responses and the severity and outcome of the disease (Li *et al.* 2021). HA is the primary target protein that produces neutralizing antibodies against AIVs by B cells. Subunit vaccines based on HA proteins have demonstrated robust immune-protective effects in both humans and animals (Du *et al.* 2011; Liu *et al.* 2013; Cummings *et al.* 2014). In the HA protein, the HA1 structural domain contains a high concentration of dominant epitopes, making it a crucial target for the development of influenza vaccines.

$CD4^+$ T cells are a critical type of immune cell that can adopt Th1 or Th2 phenotypes and coordinate immune responses (Charostad *et al.* 2023; Frey *et al.* 2023). The Th1 response activates cytotoxic $CD8^+$ T lymphocytes, natural killer cells and macrophages, while the Th2 response is essential for activating B cells, promoting homologous transformation, affinity maturation, and producing antibodies that can neutralize external pathogens (Ekkens *et al.* 2007). Influenza-specific memory $CD4^+$ T cells play a critical role in antibody production. They also have additional functions, such as expediting the recruitment of innate effector cells to the lungs and assisting in the regulation and repair of damaged cells and tissues (Strutt *et al.* 2010). These $CD4^+$ T cells are particularly important in mitigating the damage caused by severe inflammatory responses associated with highly pathogenic influenza viruses (Arpaia *et al.* 2015; Egarnes and Gosselin 2018). Another defense mechanism against viruses involves activated cytotoxic T lymphocytes (CTLs), which release enzymes that induce apoptosis and eliminate virus-infected cells to prevent further viral production (Price *et al.* 2005; Kreijtz *et al.* 2011). T-cell epitopes specific to influenza A virus primarily recognize antigenic sites within conserved internal proteins (Clemens *et al.* 2018). There has been limited progress in identifying T-cell epitopes associated with the HA protein, with most studies focusing on human-origin H1N1, H2N2, and H3N2 subtypes of IAV (Graham *et al.* 1998; Tenbusch *et al.* 2010; Knowlden *et al.* 2019; Rattan *et al.* 2019). Unfortunately, research on T cell epitopes associated with HA proteins of other subtypes, such as H5, H7, and H9 avian-origin IAVs, is relatively scarce.

In this study, we investigated the characteristics of the H9N2 subtype of AIV using genetic evolution and serological experiments. Representative viruses were selected, and peptides were synthesized based on their HA1 amino acid sequences. T-cell and B-cell epitopes of HA1 with broad reactivity within the H9 subtype were identified using peptide screening.

2. Materials and methods

2.1. Viruses, sera, and cells

H9N2 subtype AIVs A/goose/Jiangsu/JY100405C/2018 (JY100405C), A/chicken/Jiangsu/JY040218C/2019 (JY040218C), and A/chicken/Jiangsu/YX4JC5/2019 (YX4JC5) were isolated from East China between 2018 and 2019 and purified using a plaque assay. The additional 14 strains of the H9N2 subtype AIV were selected and used in this study (Appendix A) (Zhang *et al.* 2023). All viruses were cultured in 9–11-d-old embryonated SPF chicken eggs at 37°C, and allantoic fluid was collected at 72 h post-inoculation. Sera against H9N2 subtype AIVs were generated by immunizing 3-wk-old SPF chickens with an inactivated virus and an oil adjuvant. Sera for other AIV subtypes were previously prepared (Wang *et al.* 2021) and stored at −70°C (Appendix B). Madin–Darby canine kidney (MDCK) cells were cultured in Minimum Essential Medium (MEM) (HyClone, UT, USA) containing 10% fetal bovine serum (FBS) (HyClone) at 37°C and 5% CO_2.

2.2. Phylogenetic and amino acid conservation analysis

Genetic evolution analysis of 17 H9N2 AIVs was performed

using IQ-TREE (v.1.6.8) (Trifinopoulos *et al.* 2016). Visualization was performed using ITOL (v.6.5.2) (https://itol.embl.de/), wherein the key antigenic sites of the HA protein underwent multiple sequence alignments and were correlated with the evolutionary tree (Letunic and Bork 2021). Inter-branch genetic distances were calculated using MEGA5.0.

2.3. Serological assays

The HI and MN assays were performed for antigen analysis (Spackman 2020). For HI assays, the serum was gradually diluted in 2-fold increments, beginning with 25 μL, followed by the addition of 25 μL of 4 units of HA antigen. After incubating at 37°C for 15 min, 50 μL of 1% chicken red blood cells were introduced, and the mixture was further incubated at 37°C for 20 min. The highest dilution of serum that completely inhibited hemagglutination was represented by the HI titer.

MDCK cells were used for the MN assay, as described previously (Steel *et al.* 2010). The serum was heat-inactivated at 56°C for 30 min, and then a 10-fold serial dilution was conducted in MEM base culture medium. Then, 100 μL of the diluted serum was added to each well of a 96-well plate, along with 100 μL of a virus-working solution containing 2,000 $TCID_{50}$ mL^{-1}, and the serum-virus mixture was incubated at 37°C for 1 h. The serum-antibody mixture was then inoculated into a 96-well plate containing MDCK cells at a density of 2×10^4 cells per well and incubated at 37°C in a 5% CO_2 incubator for adsorption for 1 h. Once the adsorbed infected cell plate was washed thrice with PBS, 100 μL of MEM base culture medium containing 2 μg mL^{-1} TPCK trypsin was added, and the cells were cultured at 37°C and 5% CO_2. After 72 h, hemagglutination assay was performed to determine the number of positive wells. OmicStudio tools (https://www.omicstudio.cn) were used to create Heatmap Plots, while antigenic cartography (http://www.antigenic-cartography.org) was used to calculate antigenic distances (Smith *et al.* 2004).

2.4. Microarray experiment

Based on the HA1 protein amino acid sequences, a set of 55 peptides was designed with each adjacent pair overlapping 10 amino acids. The peptides were synthesized using GenScript (Nanjing, China). Of the 55 peptides, 43 were successfully synthesized and 12 were synthetic failures (Appendix C). Synthetic peptides were sampled on iPDMS, a modified silica gel film obtained from SJ Biomaterials, Suzhou, China. The microarray workflow was largely based on the methodology used in previous studies (Lu *et al.* 2015). Serum samples were analyzed using a peptide microarray. Samples were diluted in serum dilution buffer at a 1:50 ratio and added to the microarray wells. They were incubated for 30 min on a shaker at 37°C. The microarray chips were washed 3 times with TBST and dried on absorbent paper. Next, a solution of HRP-conjugated goat anti-chicken IgY was added to each well and incubated for an additional 30 min on a shaker at 37°C. After 3 additional washes, a chemiluminescent substrate was added to each well. Chemiluminescent signals were captured using the charge-coupled device camera of the imaging system and saved in TIFF-format files. GenePix Pro software (version 6.0) was used to process the chemiluminescence intensity of each peptide. The intensity was converted into signal-to-noise ratio (SNR), and a positive response was considered when SNR≥2.

2.5. Immune serum preparation and immunoprotection experiment

After peptide chip screening, broad-spectrum peptides were selected. These peptides were synthesized and coupled with bovine serum albumin (BSA) using GenScript (Nanjing, China). Next, we immunized 3-wk-old SPF chickens in groups of 5 using coupled BSA-peptide complexes. Booster immunization was administered 14 d after the primary immunization, and serum samples were collected at 14-d intervals for ELISA, HI, and MN assays to measure antibody levels. Fourteen days after the booster immunization, chickens were intranasally challenged with JY040218C at a dose of 10^6 EID_{50} per chicken. We collected throat and cloacal swabs on days 3, 5, and 7 post-challenge, and inoculated SPF chicken embryos to assess viral shedding.

2.6. Lymphocyte isolation

Three-wk-old SPF chickens were immunized with JY040218C and JY120118 from different H9N2 AIV strains. The chickens were boosted 14 d after the first vaccination. Peripheral blood was collected from the chickens on day 7 after the booster immunization. PBMCs were isolated from immunized chickens using a chicken PBMC Separation Reagent Kit (Solarbio, Beijing, China). Briefly, 10 mL of the lymphocyte separation reagent was added to the bottom of the centrifuge tube. Anticoagulant whole blood was diluted with pre-warmed PBS in equal volumes, the diluted whole blood was gently layered on top of the separation reagent, followed by centrifugation at 700×g for 30 min using a horizontal rotor at 25°C. The lymphocyte layer was aspirated and the cells were washed with 10 mL of PBS. After centrifugation at 250×g for 10 min, the cells were washed twice and cryopreserved in liquid nitrogen.

2.7. Lymphocyte proliferation

After lymphocyte resuscitation, the cell concentration was adjusted to 2×10^7 mL^{-1} in 1640 medium supplemented with 10% FBS. The cells were seeded in a 96-well plate at 2×10^6 cells per well. Following overnight incubation at 37°C, the peptides were divided into 14 groups based on their sequence number, with 3 peptides forming each group (peptides 52, 53, 54, and 55 constituted one group). These groups were then seeded onto PBMC at a concentration of 20 μg per well. After a 72 h incubation, 10 μL of CCK-8 solution was added to each well. Following a 2 h colorimetric reaction at 37°C, the OD_{450} absorbance was measured, and the proliferation rate was calculated using a formula.

Proliferation Rate=(Experimental group absorbance–Blank control absorbance)/(Control group absorbance–Blank control absorbance)×100%

Peptides with a proliferation rate surpassing 1.25 were selected from these cohorts for individual lymphocyte

stimulation to evaluate their proliferation levels.

2.8. ELISpot

Peptides with a proliferation rate of >1.25 were selected to test the induction of PBMC IFN-γ expression levels using the ELISpot Flex: Chicken IFN-γ (ALP) Assay Kit from Mabtech in Sweden. The MSIP plates from Merck in Darmstadt, Germany were activated using 15 μL of 35% ethanol and each well was washed 5 times with 200 μL of ddH_2O. The capture antibody (MT6C2) was diluted to 15 μg mL^{-1}, and 100 μL of the diluted capture antibody was added to each well for overnight coating at 4°C. Each well was then washed 5 times with 200 μL of PBS. Next, RPMI 1640 medium containing 10% FBS was added to each well and incubated for 1 h at room temperature for blocking. Next, a mixture of cells (1×10^6) and peptides (15 μg) was added to each well. Positive controls (Phorbol 12-myristate 13-acetate (PMA), 20 ng mL^{-1} and ionomycin, 1 μmol L^{-1} with cells), negative controls (unstimulated cells), and blank controls (medium only) were set up concurrently. The plates were cultured for 48 h at 37°C in a 5% CO_2 environment without disturbing the culture plate. After washing 5 times with PBS, 100 μL of biotinylated detection antibody (MT7C10-biotin) diluted to 1 μg mL^{-1} in PBS containing 0.5% BSA was added to each well for a 2 h incubation at room temperature. After 5 washes, 100 μL of streptavidin-alkaline phosphatase diluted 1:1,000 in PBS containing 0.5% BSA was added to each well for a 1 h incubation at room temperature. After 5 washes, 100 μL of BCIP/NBT-plus was added for color development until distinct spots appeared (5–30 min). The plates were then washed with water to terminate color development, and the reaction plates were air-dried in a light-avoiding environment at room temperature. Finally, spot counting and analysis were performed using an S6 Entry system (CTL, Cleveland, NY, USA).

2.9. Three-dimensional structure analysis

Peptide epitope site annotation on the structural model of the H9N2 hemagglutinin (HA) monomer (PDB ID: 1JSD) was generated using SWISS-MODEL and displayed using PyMOL software.

2.10. Statistical analysis

The statistical software GraphPad Prism 7 was used to compute the mean and standard deviation for each data group. The Student *t*-test and one-way ANOVA were used to evaluate the statistical significance of the mean differences between the various data groups. Significance levels are denoted by asterisks, with * indicating $P<0.05$, ** indicating $P<0.01$.

3. Results

3.1. H9N2 AIV exhibited variations in both genetic and antigenic characteristics

Analysis of the genetic evolution of H9N2 subtype HA proteins isolated in East China between 2017 and 2019 revealed that these isolates belonged to the h9.4.2.5 lineage. This lineage was further divided into 2 sub-branches that differed by an average genetic distance of 0.062 (Table 1). Additionally, critical antigenic sites on H9 HA (Kaverin *et al.* 2004; Peacock *et al.* 2016; Carnaccini and Perez 2020) were compared using multiple sequence alignments that correlated with the evolutionary tree. Notably, certain critical antigenic sites such as residues 90, 145, 149, 153, 164, 166, 167, 168, 197, 198, 200, and 201 (Fig. 1-A) displayed clustering.

After antibodies were prepared through H9N2 AIV immunization of SPF chickens, cross-HI and MN tests were conducted. The results of the cross-serological tests and antigenic mapping showed a clear clustering pattern in the reactivity of the sera and viruses. This pattern was consistent with the grouping observed in the genetic evolution analysis, indicating a noticeable differentiation in the amino acid sequences and antigenicity of the currently prevalent H9N2 subtype in East China (Fig. 1-C and E).

By calculating the difference in HI titers between serum-parent and serum-other strains, it was observed that the Group 1 origin sera exhibited average HI titer differences of $2^{1.06\pm1.65}$ and $2^{2.86\pm1.88}$ against Group 1 and Group 2 strains, respectively. For Group 2 sera, the average HI titer differences were $2^{3.2\pm1.87}$ and $2^{1.31\pm1.38}$ against Group 1 and Group 2 strains, respectively. Reference strains TX and F98 sera exhibited average HI titer differences of $2^{3.75\pm0.89}$ and $2^{5.33\pm1.27}$ against Group 1 and Group 2 strains, respectively (Fig. 1-B). Further, individual analyses of each strain's serum-parent and serum-other HI titer differences revealed that sera prepared from Group 2 strains WX090312, WX050801, and JY020616 and Group 1 strain JY040218C exhibited good broad-spectrum reactivity, with overall differences of <20 (a smaller difference indicating better broad-spectrum reactivity) (Table 2).

Based on the cross MN results, Group 1 sera was found to have an average neutralizing titer of $2^{13.89\pm1.4}$ and $2^{10.58\pm3.31}$ against Group 1 and Group 2 strains, respectively. The average neutralizing titers for Group 2 sera were $2^{6.70\pm2.22}$ and $2^{12.33\pm2.70}$ against Group 1 and Group 2 strains, respectively. The reference strain sera showed average neutralizing titers of $2^{9.37\pm2.07}$ and $2^{8.75\pm2.83}$ against Group 1 and Group 2 strains, respectively. It is important to note that there was a discrepancy between the MN and HI results. Sera prepared from Group 2 strains did not show robust broad-spectrum reactivity against either group, whereas sera prepared from Group 1 strains JY040128C and W6323 displayed good reactivity against most strains in both groups (Fig. 1-D).

3.2. Discovery of peptides exhibiting extensive serum binding capabilities

After conducting the cross-HI and MN assays, we used the amino acid sequences of the HA1 protein from 3 representative viruses (JY040218C, WX090312, and JY020616) as templates to create peptide fragments for 4

Table 1 Average genetic distance between selected and reference viruses after grouping

Subgroup	Intra-group average genetic distance	Inter-group average genetic distance		
		F98	TX	Group 1
Group 1	0.024	0.086	0.049	
Group 2	0.033	0.111	0.069	0.062

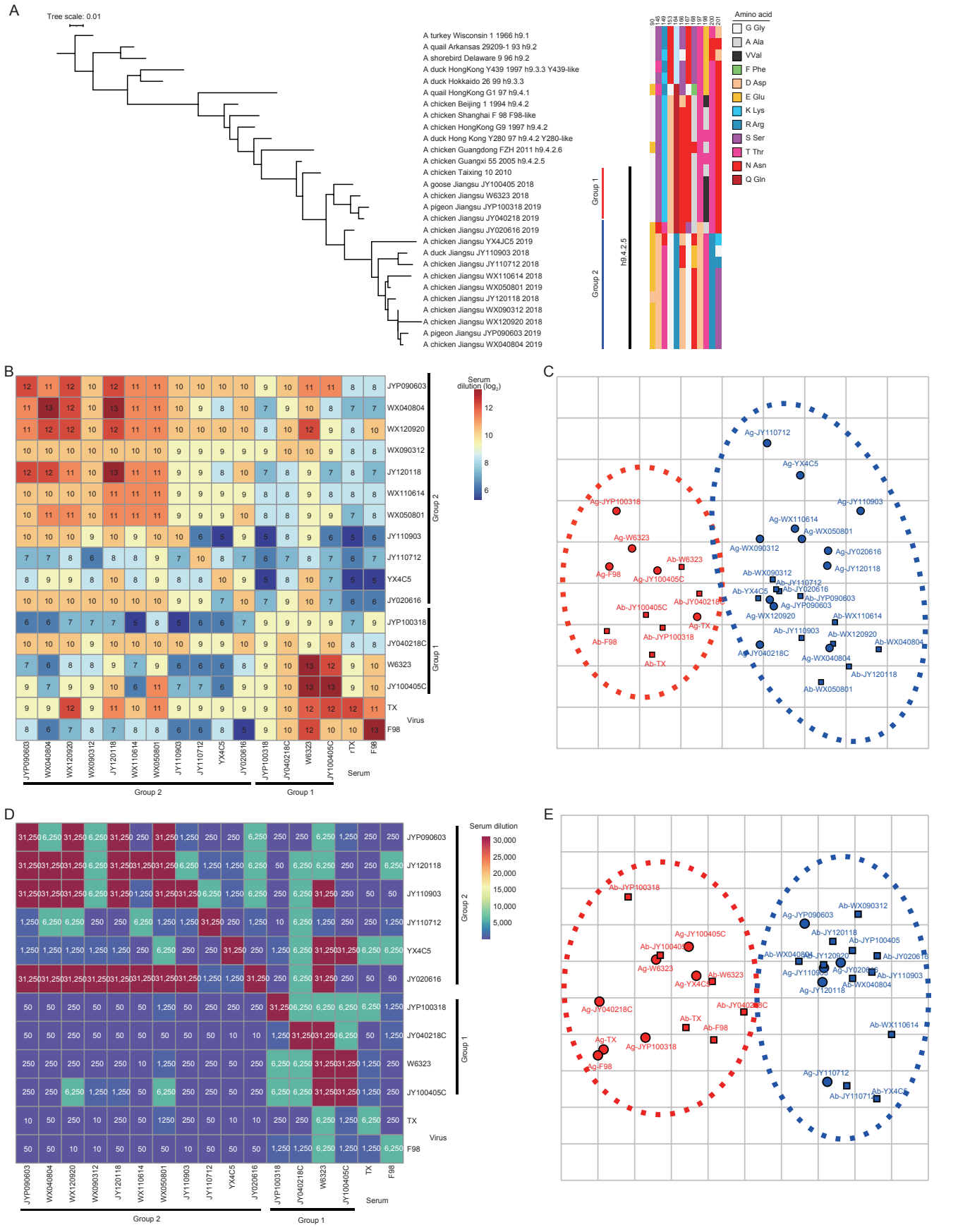


Fig. 1 Phylogenetic evolutionary and serological analysis. A, phylogenetic evolutionary of HA amino acid of several representative isolated viruses from East China, from 2017–2019. B and D, cross HI (B) and MN (D) results. C and E, antigen cartography based on the cross-HI and cross-MN assay. One unit (grid) represents a 2-fold change in the HI (C) and MN (E) assay.

Table 2 Difference values for cross-HI titers calculation results

Viruses number	Overall difference[1)]	Intra-group difference[2)]	Inter-group difference[3)]	Subgroup
JYP090603	–44	–21	–23	Group 2
WX040804	–62	–28	–34	Group 2
WX120920	–36	–17	–19	Group 2
WX090312	–17	–7	–10	Group 2
JY120118	–47	–23	–24	Group 2
WX110614	–30	–10	–20	Group 2
WX050801	–16	–7	–9	Group 2
JY110903	–27	–10	–17	Group 2
JY110712	–29	–12	–17	Group 2
YX4C5	–33	–17	–16	Group 2
JY020616	–19	–7	–12	Group 2
JYP100318	–20	0	–20	Group 1
JY040218C	–16	–1	–15	Group 1
W6323	–46	–10	–36	Group 1
JY100405C	–67	–12	–55	Group 1
TX	–73	–17	–56	Group 1
F98	–80	–17	–63	

[1)] Overall difference=Sum of all strain HI titers–HI titer of the current serum against the mother strain.
[2)] Intra-group difference=HI titers of other strains within the same group–HI titer of the current serum against the mother strain.
[3)] Inter-group difference=HI titers of all strains from different groups–HI titer of the current serum against the mother strain.

peptide microarray. We tested these peptides using sera from various sources including different AIV subtypes (Appendices B and C). Our research revealed that the 4 principal regions demonstrated broad-spectrum reactivity, specifically, segments 2/3, 20/21, 26, and 29/30/31 (Fig. 2-A). Among the 46 sera samples from H9 subtype AIVs (Appendix D), the response rates for these peptide fragments were as follows: H9-31 91.30% (42/46), H9-30 89.13% (41/46), H9-3 76.08% (35/46), H9-29 69.56% (32/46), H9-26 58.69% (27/46), H9-20 56.52% (26/46), H9-21 54.34% (25/46), and H9-2 47.82% (22/46). In addition, H9-26 had a cross-reactivity against the H3 serum, H9-29 had a cross-reactivity against the H7 serum, while H9-31 had a cross-reactivity against the H4 and H5 sera. The other selected peptides had no cross-reactivity against the sera against different subtype AIVs (Fig. 2-B; Appendix E).

Additionally, we analyzed the conservation of amino acid residues in H9-3, H9-21, H9-26, and H9-30 from 2016–2021. Our results showed that all the peptides exhibited high levels of conservation, with conservation rates exceeding 96% at each position in both H9-3 and H9-21. For H9-26, conservation at other positions was >90%, except at position 260 (K: 82.56%; R: 13.27%). Similarly, for H9-30, conservation at other positions exceeded 96%, except at position 302 (I: 80.25%, V: 18.88%) (Fig. 2-C and D). Our simulation analysis of the tertiary structure of the HA protein indicated that the H9-21 peptide was located proximate to the receptor-binding site, whereas the other 3 regions were located within the stem region of the HA protein (Fig. 2-G).

3.3. Peptides H9-21, H9-26, and H9-30 effectively elicit the production of antibodies

Peptides H9-3, H9-21, H9-26, and H9-30 were coupled with BSA and used to immunize SPF chickens to generate antibodies. ELISA results showed that H9-26 was the most effective at stimulating antibody production against the corresponding epitope, with the highest levels reached after boost vaccination. H9-21 and H9-30 also induced antibody production to a lesser extent but still showed a significant difference compared with the PBS group (P<0.01). However, immunization with H9-3 induced antibody levels, which were not significantly different from those in the PBS group (Fig. 3-B). Indirect immunofluorescence assay results revealed that sera against H9-21, H9-26, and H9-30 reacted with Group 1 strain JY040218C and Group 2 strain JY120118, whereas sera against H9-3 failed to react with Group 2 strain JY120118 (Fig. 3-C).

Although immunization with peptides coupled with BSA did not provide complete protection against the H9N2 subtype AIV challenge, vaccination with H9-26 and H9-30 peptides reduced viral shedding in the trachea of challenged chickens compared to the PBS group (Table 3).

3.4. Peptides H9-15, H9-22, and H9-23 activate lymphocytes

Lymphocytes were isolated from the chickens immunized with JY040218C or JY120118. The lymphocytes were then stimulated with 14 different peptides. The results showed that lymphocytes from chickens immunized with JY040218C exhibited significant proliferation when stimulated with peptides from Groups 4, 7, 8, 11, 12, 13, and 14. Similarly, lymphocytes from chickens immunized with JY120118 showed effective proliferation when stimulated with peptides from Groups 4, 6, 7, 8, 11, and 14 (Fig. 4-A and B). Further analysis was conducted by stimulating lymphocytes with individual peptides from the positive stimulus groups. The results showed that peptides H9-12, H9-15, H9-22, H9-23, H9-29, H9-49, and H9-52 effectively stimulated lymphocyte proliferation in individuals immunized with JY040218C. In contrast, lymphocytes from JY120118-immunized chickens exhibited effective proliferation in response to the peptides H9-12, H9-13, H9-21, H9-22, H9-24, H9-29, H9-41, H9-46, H9-48, H9-52, H9-53, and H9-54. Collectively, peptides H9-12, H9-22, H9-29, and H9-52 effectively stimulated the proliferation of lymphocytes from chickens immunized with different strains from the respective groups (Fig. 4-C and D).

ELISpot was conducted to determine the expression levels of IFN-γ in lymphocytes after being stimulated by various peptides. Seven groups of peptides with individual amino acid differences were chosen as isomeric peptides. The results indicated that peptides H9-15, H9-22, and H9-23, along with their corresponding isomeric peptides, could effectively stimulate the expression of IFN-γ in lymphocytes immunized with viruses from different groups (Fig. 4-E and F; Appendix F). These findings suggested that peptides H9-15, H9-22, and H9-23 have the potential to act as T-cell epitopes.

4. Discussion

This study conducted a genetic evolutionary analysis of the HA amino acid sequences of the H9N2 subtype isolates from East China between 2017 and 2019. The results showed that similar to other regions in the country, the h9.4.2.5 lineage

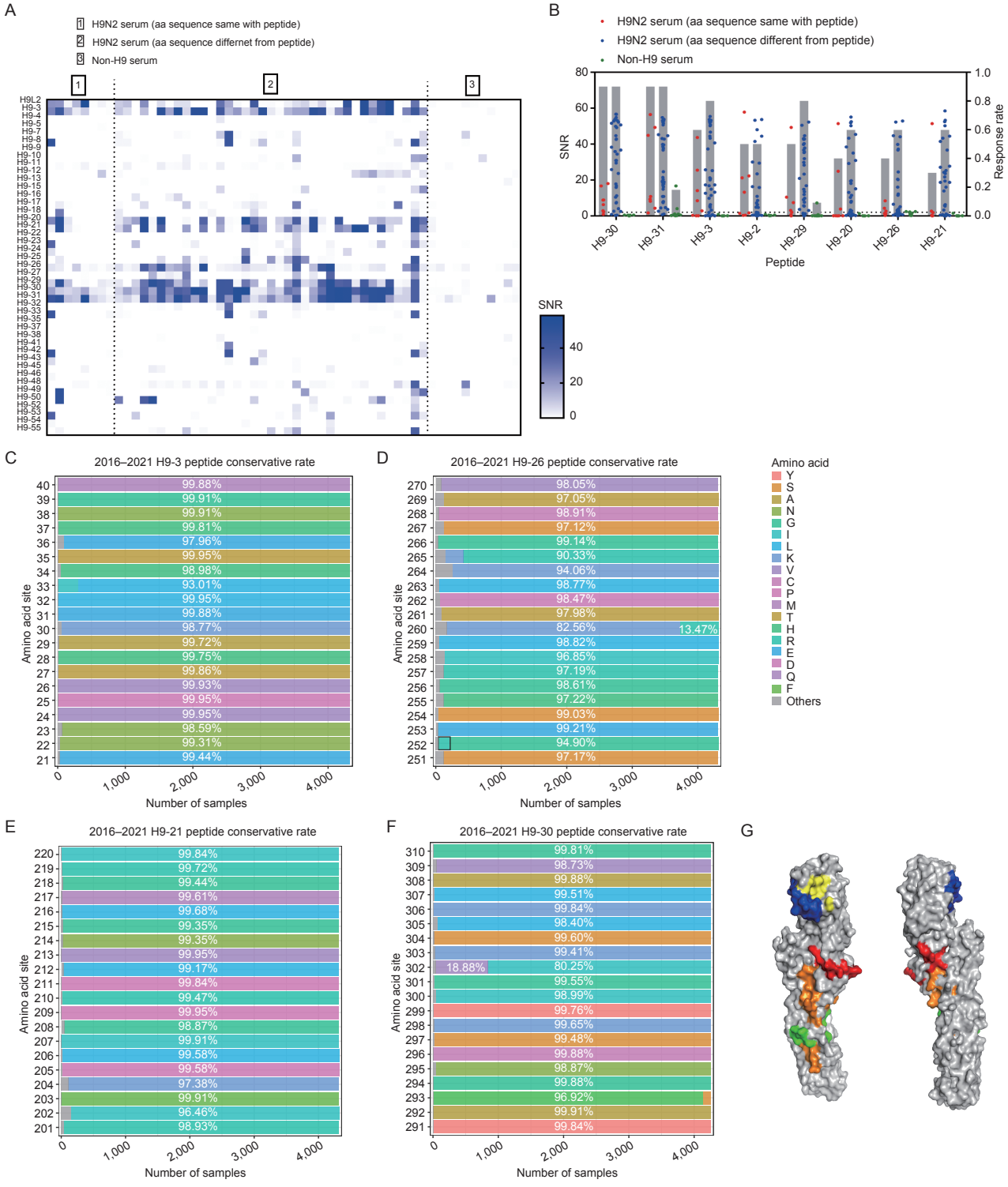


Fig. 2 Microarray and conservation analysis of the peptides. A, the signal-to-noise ratios (SNRs) and response rate of the reactions between antisera against all H9 peptides. B, comparison of SNR values and response rates for peptides with higher responsiveness. C–F, conservative analysis of amino acid positions of peptides H9-3, H9-21, H9-26, and H9-30 from 2016 to 2021. G, projection of peptides H9-3, H9-21, H9-26, and H9-30 tertiary structure. Yellow represents the receptor binding region, green represents peptide H9-3, blue represents peptide H9-21, red represents peptide H9-26, and orange represents peptide H9-30.

was the dominant virus in East China (Zhang *et al.* 2021; Liu *et al.* 2022). Further investigation revealed that this lineage can be divided into 2 distinct groups, consistent with previous research (Zhang *et al.* 2023). Our study identified these groups as Groups 1 and 2, which is consistent with Wang's clades 15 and 16 (Wang *et al.* 2023) and Yan's subgroups II and III (Yan *et al.* 2022). A comparative analysis of the 12 reported key antigenic site amino acid patterns also showed consistent differentiation, indicating that the genetic evolution of HA formed 2 distinct groups (Wang *et al.* 2023). Overall,

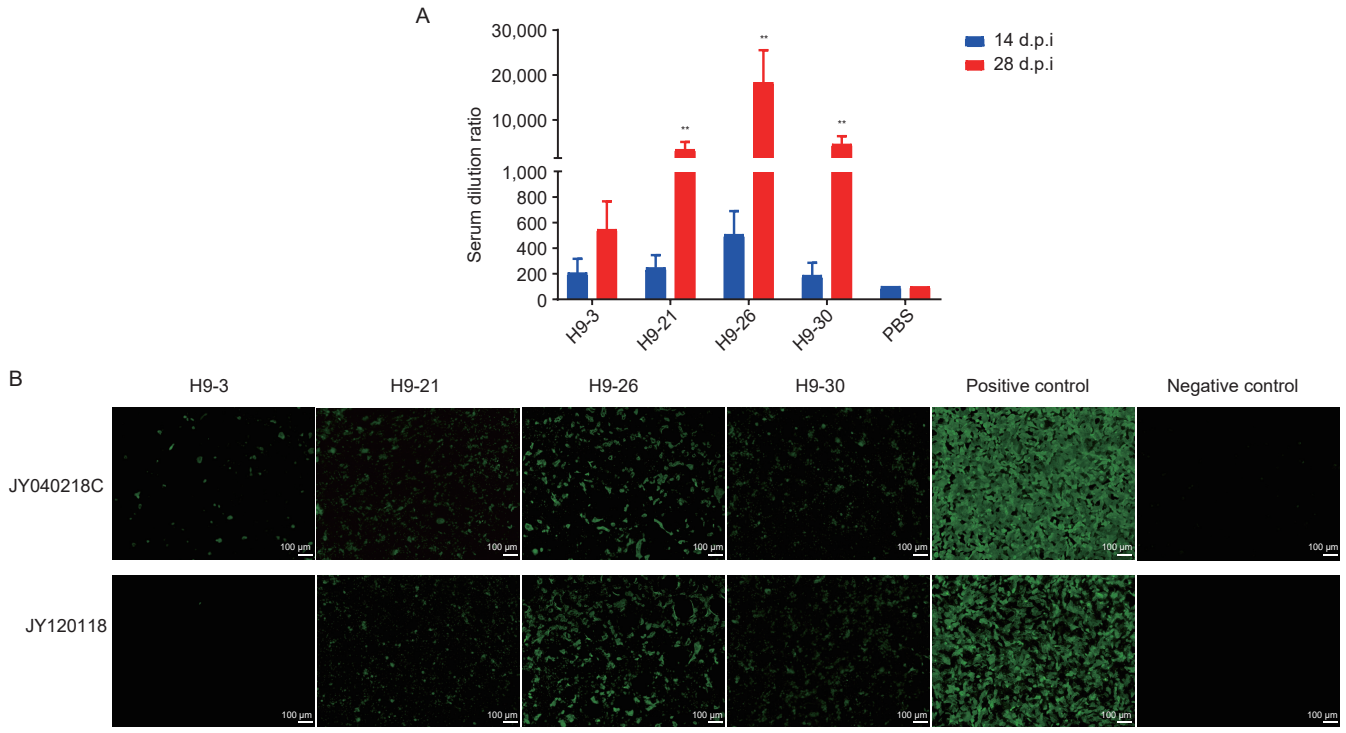


Fig. 3 Determination of the inductive antibody level abilities of peptides H9-3, H9-21, H9-26, and H9-30. A, ELISA determination of peptide-induced antibody levels. B, reactivity of peptide-induced antibodies against H9N2 subtype viruses from different groups. Statistical significance between the peptide groups and PBS group were determined by unpaired two-tailed Student's *t*-test. Data are mean±SD. *, $P<0.05$; **, $P<0.01$. d.p.i., days post immunization.

Table 3 Protective effects of peptide immunizations

Immunization group	Challenge virus	Days post challenge (d.p.c.)[1)]					
		3		5		7	
		T	C	T	C	T	C
H9-3	JY040218C	5/5	0/5	4/5	0/5	3/5	0/5
H9-21	JY040218C	5/5	0/5	5/5	0/5	3/5	0/5
H9-26	JY040218C	5/5	0/5	3/5	0/5	2/5	0/5
H9-30	JY040218C	5/5	0/5	3/5	0/5	3/5	0/5
PBS	JY040218C	5/5	0/5	5/5	0/5	4/5	0/5

[1)] T, throat swab. C, cloacal swab. Shedding rate=Shedding number/Total number.

the genetic evolutionary findings suggested that the prevalent H9N2 subtype AIV strains in East China belong mainly to the h9.4.2.5 lineage, with significant differences in amino acid patterns at key antigenic sites. The cross-HI and MN assays yielded significant results, indicating notable antigenic differences among the H9N2 subtype AIV isolates from East China. These differences align with the observed genetic evolution, as reflected by the two-group clustering pattern, as seen in Fig. 1-A, C, and E. Interestingly, sera derived from the vaccine-referencing strains F98 and TX consistently demonstrated superior serological reactivity to the Group 1 strain in HI and MN assays (Fig. 1-B and D). This mirrors the genetic evolution analysis, in which Group 1 exhibited a closer genetic distance to the reference strains than Group 2 did. Conversely, Group 2 strains exhibited poorer HI and MN cross-reactivity than Group 1 strains, indicating ongoing differentiation within Group 2 strains. This finding is consistent with Wang's study, in which clades 15 and 16 strains also exhibited 2 distinct antigenic clusters in cross-HI results (Wang *et al.* 2023). Based on these results, we found good serological broad-spectrum reactivity in the strains JY040218C, W6323, WX090312, WX050801, and JY020616.

Currently, the research on the systematic identification of antigenic sites in the H9 HA1 protein is limited. However, previous studies have successfully utilized microarray experiments to identify specific antigenic sites on H5 and H7 subtype HA2 proteins, resulting in the development of corresponding tagged vaccine strains (Sun *et al.* 2021; Wang *et al.* 2021). Therefore, we employed a microarray method to identify antigenic sites in the H9 HA1 protein. Following serum scanning identification, peptides from the 4 regions demonstrated broad reactivity to immune sera derived from H9 subtype AIV (Fig. 2-A and B). Previous research has identified HA233 as a B-cell epitope within the HA protein, and immunized mice with a complex of HA233 and cholesterol half-succinyl succinate generated neutralizing antibodies, providing complete protection against a lethal dose challenge from the recombinant H5N1 virus (Rhee *et al.* 2012). Additionally, Peacock identified a distinct set of escape mutants within the 220 loop of the receptor-binding site of the H9N2 subtype HA (Peacock *et al.* 2016), which was encompassed within the H9-21 peptide screened in this study. We conducted a challenge protection experiment using peptide-immunized SPF chickens to determine the efficacy of the identified peptides. The experimental group showed an inhibitory effect on tracheal shedding compared to

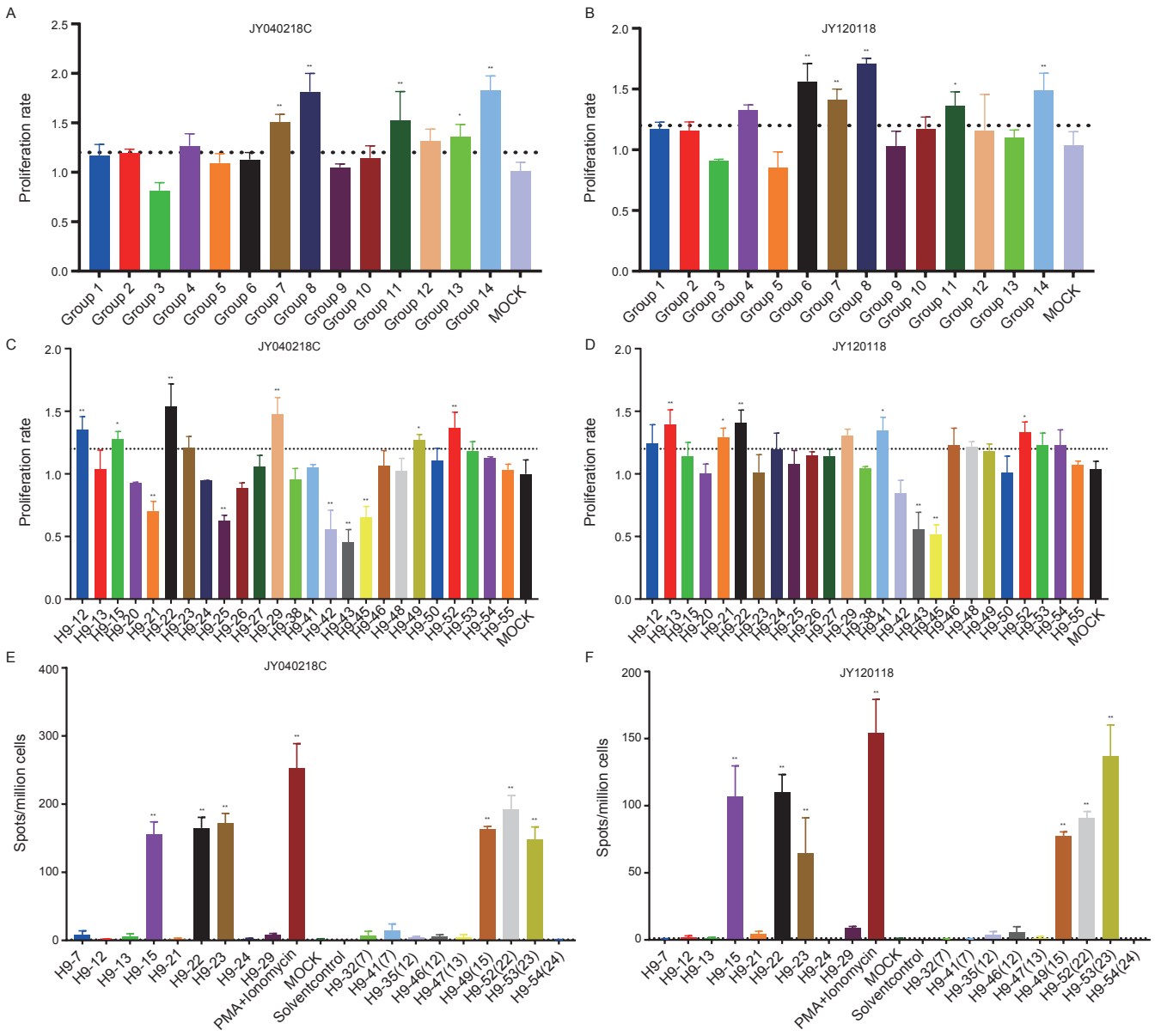


Fig. 4 Cellular immune responses induced by peptide. A and B, group peptide stimulation PBMC after immunization with JY040218C and JY120118. C and D, single peptide stimulation PBMC after immunization with JY040218C and JY120118. E and F, JY040218C and JY120118 immunized peripheral blood lymphocytes were isolated and subjected to ELISpot assay to quantify the number of cells secreting IFN-γ. Data are mean±SD. Statistical significance between the peptide groups and MOCK group were determined by one-way ANOVA. *, $P<0.05$; **, $P<0.01$.

the control group. However, all 4 peptide-immunized groups, including peptide H9-21, which has been reported to have superior immune protective effects, failed to achieve complete protection, likely due to the limited immunogenicity of single linear peptides. Therefore, although our study highlights the potential value of these peptides, further exploration of suitable immunization strategies and delivery vehicles is required to optimize their efficacy.

After analyzing the tertiary domain and conservation of amino acids of B cell epitopes, it was noted that, except for 3 epitopes in the stem region (H9-3, H9-26, and H9-30), H9-21 near the HA receptor-binding site exhibited highly conserved characteristics. The B cell epitope H9-21 located in the HA receptor binding domain may interrupt the virus replication by inducing antibodies that prevent virus-receptor binding, while H9-26 and H9-30 located in the HA stem may block the virus replication by inducing antibodies that prevent membrane fusion (Lim *et al.* 2024). Rhee discovered that direct immunization with an inactivated whole virus did not effectively stimulate the production of antibodies corresponding to HA233, indicating that although H9-21 is in the HA1 head, it can be considered a subdominant antigenic epitope that is less vulnerable to antibody generation pressure during traditional vaccine immunization methods. Consequently, they maintain a level of conservation similar to that of stem epitopes (Rhee *et al.* 2012). This discovery highlights the immunological importance of H9-21, particularly in the development of vaccines against H9 subtype AIVs. However, further research is necessary to determine the best way to use this finding to enhance vaccine

efficacy, combination of multiple B-cell epitopes or both B-cell and T-cell epitopes in vaccine design might improve its protective efficacy.

Research on AIV HA-associated T-cell antigenic epitopes in avian hosts is limited. To address this, we screened vaccinated chickens to identify the AIV H9 HA T-cell epitopes. Our results showed that peptides H9-15, H9-22, and H9-23, along with their isomeric peptides, effectively stimulated the expression of IFN-γ in PBMC from chickens after immunization with strains from different sources (Fig. 4-E and F; Appendix E). Knowlden and Richards also conducted studies to identify T-cell epitopes for H1N1-derived HA proteins in mice expressing MHC II molecules and in HLA-DR transgenic mice, respectively. Interestingly, the HA p28162–178 and HA232-249 (Richards *et al.* 2007; Knowlden *et al*. 2019) peptides identified in their studies showed high sequence identity with the H9-15 and H9-22 peptides identified in our study. These conserved T-cell epitopes may activate $CD4^+$ T cell and $CD8^+$ cytotoxic T cells response, which can induce cross-reactivity with a variety of influenza A viruses of different subtypes (Kreijtz *et al*. 2011).

5. Conclusion

Overall, between 2017 and 2019, a clustering phenomenon of H9N2 subtype AIV was observed in East China in terms of serology and genetic evolution. We screened 5 strains of viruses with good serological broad-spectrum reactivity based on HI and MN results and identified 5 novel cell epitopes of the H9 HA1 protein using microarray and peptide scanning techniques. These findings can be utilized in vaccine design and detection of H9N2 AIVs.

Acknowledgements

This work was supported by the National Key Research and Development Program of China (2021YFD1800202), the National Natural Science Foundation of China (3237042 and 32172942), the "Jie Bang Gua Shuai" Project at Yangzhou University, China (YZUXK202316), the Agricultural Science and Technology Independent Innovation Fund of Jiangsu Province, China (SCX[22]3547), the Outstanding Technological Innovation Team of College and University at Jiangsu Province, China ([2021] NO.1) and a project funded by the Priority Academic Program Development of Jiangsu Higher Education, China (PAPD).

Declaration of competing of interest

These authors declare that they have no conflict of interest.

Declaration of generative AI and AI-assisted technologies in the writing process

During the preparation of this manuscript, the authors used ChatGPT 4.0 to assist in improving the clarity and readability of the language. All content generated was carefully reviewed and revised by the authors as necessary, and the authors take full responsibility for the final content of the article.

Ethical approval

Three-wk-old specific-pathogen-free (SPF) chickens were purchased from the Shandong Poultry Research Institute, China. All *in vivo* animal experiments were performed in negative-pressure isolators at the authorized animal biosafety level 2 (ABSL-2) facility at Yangzhou University, approved by the Jiangsu Administrative Committee for Laboratory Animals, and complied with the guidelines for laboratory animal welfare and ethics of the Jiangsu Administrative Committee for Laboratory Animals (Permission number: SYXKSU-2016-0020).

Appendices associated with this study are available at https://doi.org/10.1016/j.jia.2024.07.005

References

Arpaia N, Green J A, Moltedo B, Arvey A, Hemmers S, Yuan S, Treuting P M, Rudensky A Y. 2015. A distinct function of regulatory T cells in tissue protection. *Cell*, **162**, 1078–1089.

Belser J A, Sun X, Brock N, Pappas C, Pulit-Penaloza J A, Zeng H, Jang Y, Jones J, Carney P J, Chang J, Long N V, Diep N T, Thor S, Di H, Yang G, Cook P W, Creager H M, Wang D, Mcfarland J, Dong P V, *et al.* 2020. Genetically and antigenically divergent influenza a(h9n2) viruses exhibit differential replication and transmission phenotypes in mammalian models. *Journal of Virology*, **94**, e00451–20.

Bi Y, Li J, Li S, Fu G, Jin T, Zhang C, Yang Y, Ma Z, Tian W, Li J, Xiao S, Li L, Yin R, Zhang Y, Wang L, Qin Y, Yao Z, Meng F, Hu D, Li D, *et al.* 2020. Dominant subtype switch in avian influenza viruses during 2016–2019 in China. *Nature Communications*, **11**, 5909.

Cao Y, Liu H, Liu D, Liu W, Luo T, Li J. 2022. Hemagglutinin gene variation rate of H9N2 avian influenza virus by vaccine intervention in China. *Viruses*, **14**, 1043.

Carnaccini S, Perez D R. 2020. H9 influenza viruses: An emerging challenge. *Cold Spring Harbor Perspectives in Medicine*, **10**, a038588.

Charostad J, Rezaei Zadeh Rukerd M, Mahmoudvand S, Bashash D, Hashemi S M A, Nakhaie M, Zandi K. 2023. A comprehensive review of highly pathogenic avian influenza (HPAI) H5N1: An imminent threat at doorstep. *Travel Medicine and Infectious Disease*, **55**, 102638.

Chen H, Yuan H, Gao R, Zhang J, Wang D, Xiong Y, Fan G, Yang F, Li X, Zhou J, Zou S, Yang L, Chen T, Dong L, Bo H, Zhao X, Zhang Y, Lan Y, Bai T, Dong J, *et al.* 2014. Clinical and epidemiological characteristics of a fatal case of avian influenza A H10N8 virus infection: A descriptive study. *Lancet*, **383**, 714–721.

Chen J M, Sun Y X, Chen J W, Liu S, Yu J M, Shen C J, Sun X D, Peng D. 2009. Panorama phylogenetic diversity and distribution of type A influenza viruses based on their six internal gene sequences. *Virology Journal*, **6**, 137.

Clemens E B, Van De Sandt C, Wong S S, Wakim L M, Valkenburg S A. 2018. Harnessing the power of T cells: The promising hope for a universal influenza vaccine. *Vaccines* (Basel), **6**, 18.

Cummings J F, Guerrero M L, Moon J E, Waterman P, Nielsen R K, Jefferson S, Gross F L, Hancock K, Katz J M, Yusibov V. 2014. Safety and immunogenicity of a plant-produced recombinant monomer hemagglutinin-based influenza vaccine derived from influenza A (H1N1)pdm09 virus: A Phase 1 dose-escalation study in healthy adults. *Vaccine*, **32**, 2251–2259.

Du L, Leung V H, Zhang X, Zhou J, Chen M, He W, Zhang H Y, Chan C C, Poon V K, Zhao G, Sun S, Cai L, Zhou Y, Zheng B J, Jiang S. 2011. A recombinant vaccine of H5N1 HA1 fused with foldon and human IgG Fc induced complete cross-clade protection against divergent H5N1 viruses. *PLoS ONE*, **6**, e16555.

Egarnes B, Gosselin J. 2018. Contribution of regulatory T cells in nucleotide-binding oligomerization domain 2 response to influenza virus infection. *Frontiers in Immunology*, **9**, 132.

Ekkens M J, Shedlock D J, Jung E, Troy A, Pearce E L, Shen H, Pearce E J. 2007. Th1 and Th2 cells help CD8 T-cell responses. *Infection and Immunity*, **75**, 2291–2296.

Frey S S, Versage E, Van Twuijver E, Hohenboken M. 2023. Antibody responses against heterologous H5N1 strains for an MF59-adjuvanted cell culture-derived H5N1 (aH5n1c) influenza vaccine

in adults and older adults. *Human Vaccines & Immunotherapeutics*, **19**, 2193119.
Graham C M, Smith C A, Thomas D B. 1998. Novel diversity in Th1, Th2 type differentiation of hemagglutinin-specific T cell clones elicited by natural influenza virus infection in three major haplotypes (H–$2^{b,d,k}$). *The Journal of Immunology*, **161**, 1094–1103.
Guo Y J, Krauss S, Senne D A, Mo I P, Lo K S, Xiong X P, Norwood M, Shortridge K F, Webster R G, Guan Y. 2000. Characterization of the pathogenicity of members of the newly established H9N2 influenza virus lineages in Asia. *Virology*, **267**, 279–288.
Kaverin N V, Rudneva I A, Ilyushina N A, Lipatov A S, Krauss S, Webster R G. 2004. Structural differences among hemagglutinins of influenza A virus subtypes are reflected in their antigenic architecture: Analysis of H9 escape mutants. *Journal of Virology*, **78**, 240–249.
Knowlden Z A G, Richards K A, Moritzky S A, Sant A J. 2019. Peptide epitope hot spots of CD4 T cell recognition within influenza hemagglutinin during the primary response to infection. *Pathogens*, **8**, 220.
Kreijtz J H C M, Fouchier R A M, Rimmelzwaan G F. 2011. Immune responses to influenza virus infection. *Virus Research*, **162**, 19–30.
Letunic I, Bork P. 2021. Interactive Tree of Life (iTOL) v5: An online tool for phylogenetic tree display and annotation. *Nucleic Acids Research*, **49**, W293–W296.
Li Y, Ma M L, Lei Q, Wang F, Hong W, Lai D Y, Hou H, Xu Z W, Zhang B, Chen H, Yu C, Xue J B, Zheng Y X, Wang X N, Jiang H W, Zhang H N, Qi H, Guo S J, Zhang Y, Lin X, *et al.* 2021. Linear epitope landscape of the SARS-CoV-2 Spike protein constructed from 1,051 COVID-19 patients. *Cell Reports*, **34**, 108915.
Li Y T, Linster M, Mendenhall I H, Su Y C F, Smith G J D. 2019. Avian influenza viruses in humans: Lessons from past outbreaks. *British Medical Bulletin*, **132**, 81–95.
Liang L, Bai Y, Huang W, Ren P, Li X, Wang D, Yang Y, Gao Z, Tang J, Wu X, Gao S, Guo Y, Hu M, Wang Z, Wang Z, Ma H, Li J. 2024. Genetic and biological properties of H9N2 avian influenza viruses isolated in central China from 2020 to 2022. *Journal of Integrative Agriculture*, **23**, 2778-2791.
Lim C M L, Komarasamy T V, Adnan N, Radhakrishnan A K, Balasubramaniam V. 2024. Recent advances, approaches and challenges in the development of universal influenza vaccines. *Influenza and Other Respiratory Viruses*, **18**, e13276.
Liu D, Shi W, Gao G F. 2014. Poultry carrying H9N2 act as incubators for novel human avian influenza viruses. *Lancet*, **383**, 869.
Liu G, Zhang F, Shi J, Tian G, Chen H, Yu K, Meng Q. 2013. A subunit vaccine candidate derived from a classic H5N1 avian influenza virus in China protects fowls and BALB/c mice from lethal challenge. *Vaccine*, **31**, 5398–5404.
Liu Q, Zhao L, Guo Y, Zhao Y, Li Y, Chen N, Lu Y, Yu M, Deng L, Ping J. 2022. Antigenic evolution characteristics and immunological evaluation of H9N2 avian influenza viruses from 1994–2019 in China. *Viruses*, **14**, 726.
Liu S, Ji K, Chen J, Tai D, Jiang W, Hou G, Chen J, Li J, Huang B. 2009. Panorama phylogenetic diversity and distribution of Type A influenza virus. *PLoS ONE*, **4**, e5022.
Lu Y, Li Z, Teng H, Xu H, Qi S, He J, Gu D, Chen Q, Ma H. 2015. Chimeric peptide constructs comprising linear B-cell epitopes: Application to the serodiagnosis of infectious diseases. *Scientific Reports*, **5**, 13364.
Peacock T, Reddy K, James J, Adamiak B, Barclay W, Shelton H, Iqbal M. 2016. Antigenic mapping of an H9N2 avian influenza virus reveals two discrete antigenic sites and a novel mechanism of immune escape. *Scientific Reports*, **6**, 18745.
Peacock T H P, James J, Sealy J E, Iqbal M. 2019. A global perspective on H9N2 avian influenza virus. *Viruses*, **11**, 620.
Price G E, Huang L, Ou R, Zhang M, Moskophidis D. 2005. Perforin and Fas cytolytic pathways coordinately shape the selection and diversity of $CD8^+$ T-cell escape variants of influenza virus. *Journal of Virology*, **79**, 8545–8559.
Pu J, Wang S, Yin Y, Zhang G, Carter R A, Wang J, Xu G, Sun H, Wang M, Wen C, Wei Y, Wang D, Zhu B, Lemmon G, Jiao Y, Duan S, Wang Q, Du Q, Sun M, Bao J, *et al.* 2015. Evolution of the H9N2 influenza genotype that facilitated the genesis of the novel H7N9 virus. *Proceedings of the National Academy of Sciences of the United States of America*, **112**, 548–553.
Rattan A, Richards K A, Knowlden Z A G, Sant A J. 2019. Protein vaccination directs the $CD4^+$ T cell response toward shared protective epitopes that can be recalled after influenza virus infection. *Journal of Virology*, **93**, e00947–19.
Rhee J W, Kim D, Park B K, Kwon S, Cho S, Lee I, Park M S, Seo J N, Kim Y S, Choi H S, Lee Y, Kwon H J. 2012. Immunization with a hemagglutinin-derived synthetic peptide formulated with a CpG-DNA-liposome complex induced protection against lethal influenza virus infection in mice. *PLoS ONE*, **7**, e48750.
Richards K A, Chaves F A, Krafcik F R, Topham D J, Lazarski C A, Sant A J. 2007. Direct *ex vivo* analyses of HLA-DR1 transgenic mice reveal an exceptionally broad pattern of immunodominance in the primary HLA-DR1-restricted CD4 T-cell response to influenza virus hemagglutinin. *Journal of Virology*, **81**, 7608–7619.
Smith D J, Lapedes A S, De Jong J C, Bestebroer T M, Rimmelzwaan G F, Osterhaus A D M E, Fouchier R a M. 2004. Mapping the antigenic and genetic evolution of influenza virus. *Science*, **305**, 371–376.
Spackman E. 2020. *Animal Influenza Virus*: *Methods and Protocols*. Humana Press, New York. pp. 11–28.
Steel J, Lowen A C, Wang T T, Yondola M, Gao Q, Haye K, García-Sastre A, Palese P. 2010. Influenza virus vaccine based on the conserved hemagglutinin stalk domain. *mBio*, **1**, e00018–10.
Strutt T M, Mckinstry K K, Dibble J P, Winchell C, Kuang Y, Curtis J D, Huston G, Dutton R W, Swain S L. 2010. Memory $CD4^+$ T cells induce innate responses independently of pathogen. *Nature Medicine*, **16**, 558–564.
Sun Z, Wang Q, Li G, Li J, Chen S, Qin T, Ma H, Peng D, Liu X. 2021. Development of an inactivated h7n9 subtype avian influenza serological diva vaccine using the chimeric HA epitope approach. *Microbiology Spectrum*, **9**, e0068721.
Tenbusch M, Grunwald T, Niezold T, Storcksdieck Genannt Bonsmann M, Hannaman D, Norley S, Uberla K. 2010. Codon-optimization of the hemagglutinin gene from the novel swine origin H1N1 influenza virus has differential effects on $CD4^+$ T-cell responses and immune effector mechanisms following DNA electroporation in mice. *Vaccine*, **28**, 3273–3277.
Trifinopoulos J, Nguyen L T, Von Haeseler A, Minh B Q. 2016. W-IQ-TREE: A fast online phylogenetic tool for maximum likelihood analysis. *Nucleic Acids Research*, **44**, W232-W235.
Wang Q, Sun Z, Li J, Qin T, Ma H, Chen S, Peng D, Liu X. 2021. Identification of a universal antigen epitope of influenza A virus using peptide microarray. *BMC Veterinary Research*, **17**, 22.
Wang X, Liu K, Guo Y, Pei Y, Chen X, Lu X, Gao R, Chen Y, Gu M, Hu J, Liu X, Hu S, Jiao X A, Liu X, Wang X. 2023. Emergence of a new designated clade 16 with significant antigenic drift in hemagglutinin gene of H9N2 subtype avian influenza virus in eastern China. *Emerging Microbes & Infections*, **12**, 2249558.
Yan W, Cui H, Engelsma M, Beerens N, Van Oers M M, De Jong M C M, Li X, Liu Q, Yang J, Teng Q, Li Z. 2022. Molecular and antigenic characterization of avian H9N2 viruses in Southern China. *Microbiology Spectrum*, **10**, e0082221.
Zhang N, Quan K, Chen Z, Hu Q, Nie M, Xu N, Gao R, Wang X, Qin T, Chen S, Peng D, Liu X. 2023. The emergence of new antigen branches of H9N2 avian influenza virus in China due to antigenic drift on hemagglutinin through antibody escape at immunodominant sites. *Emerging Microbes & Infections*, **12**, 2246582.
Zhang S, Yu J L, He L, Gong L, Hou S, Zhu M, Wu J B, Su B, Liu J, Wu G, He J. 2021. Molecular characteristics of the H9N2 avian influenza viruses in live poultry markets in Anhui Province, China, 2013 to 2018. *Health Science Reports*, **4**, e230.
Zhang X, Li Y, Jin S, Wang T, Sun W, Zhang Y, Li F, Zhao M, Sun L, Hu X, Feng N, Xie Y, Zhao Y, Yang S, Xia X, Gao Y. 2022. H9N2 influenza virus spillover into wild birds from poultry in China bind to human-type receptors and transmit in mammals *via* respiratory droplets. *Transboundary and Emerging Diseases*, **69**, 669–684.
Zhao Y R, Zhao Y Z, Liu S D, Xiao Y H, Li N, Liu K H, Meng F L, Zhao J, Liu M D, Li B Q. 2023. Phylogenetic and epidemiological characteristics of H9N2 avian influenza viruses in Shandong Province, China from 2019 to 2021. *Journal of Integrative Agriculture*, **22**, 881–896.

Executive Editor-in-Chief Dongming Zhao
Managing Editor Han Zhang